Understanding The Lead-Free Ferroelectric Material Phase Transitions Using Lattice Distortion Studies and Williamson Hall Plots

B. SIRIVENNELA[1], G PRASAD[2]
[1, 2]*Department of Physics, JNTUH University College of Engineering, Science and Technology Hyderabad*

Abstract ***Lead free piezoelectric ceramic composites (1-x) $Na_{0.5}Bi_{0.5}TiO_3$-x$SrTiO_3$ Where x=0.0-1.0 were prepared by sol-gel method. X-ray diffraction revealed the coexistence of Rhombohedral and cubic phases. This paper aims to explore the phase transition behaviour in lead-free ferroelectric materials using lattice distortion studies and Williamson-Hall (WH) plots to uncover the underlying mechanisms that influence material properties. The study will center on the use of X-ray diffraction (XRD) techniques to track changes in lattice parameters across different temperature-dependent and doping induced phase transitions. Lattice distortions, which are critical to the material's behavior, will be quantitatively analyzed to reveal how strain and crystallite size evolve during these transitions. The W-H plot of the XRD data enables separation of the strain and crystallite size contributions to the broadening of diffraction peaks.***

Index Terms- NBT, ST, Piezoelectric and Impedance.

I. INTRODUCTION

Lead based ceramics have more applications in electronics as well as in science field due to its excellent piezoelectric properties. But it lost its importance because of its tremendous influence of lead content on human health. Sodium bismuth titanate (NBT) is good ferroelectric material that can replace the lead based ferroelectrics. They are widely used in piezo as well as pyroelectric applications. NBT was first discovered and reported by smolenskii et al (1).NBT has rhombohedral structure and belongs to R3c space group. It is having high coercively (Ec=70 KV cm-1) and remananet polarization is about 38 Cμ/cm^2(2). NBT has transformation of ferroelectric phase (rhomohedral)to antiferroelectric phase(orthorhombic) at 200^0C and anti ferroelectric(orthorhombic) to the paraelectric phase(tetragonal) around 320^0C,at 540^0C it changes to cubic structure(3). Strontium titanate is a material with cubic perovskite structure and good insulating properties (4).And it is having more advantages of its incipient ferroelectricity and polar soft mode behavior (5). To modify and improve the properties of NBT many solid solutions such asNBT-BaTiO3, NBT-BiCrO3, NBT-BiAlO3 etc are prepared (6).

In the present paper, we report NBT-ST composites prepared by sol gel route and the measurements such as dielectric, piezoelectric and conductivity of all NBT-ST composites are undertaken and studied how these parameters are differ from solid solutions. Our work is aimed at an understanding on how these materials behave, especially during phase transitions, by studying their lattice distortions and using techniques like, Schearer formula, Williamson-Hall plots and Goldschmidt tolerance factor etc.

II. EXPERIMENTAL METHODS

NBT and ST powders were prepared by Sol-Gel method. For the preparation of NBT, taking the Stoichiometric proportion of $NaNO_3$ (SD fine 99.5%), $Bi(NO_3)_3$ (SD fine 99.5%), Ti (100 mesh, Aldrich 99.7%) ,H_2O_2(30%, SD fine) and Ammonia solution(25% AR grade, SD fine). Similarly for the preparation of $SrTio_3$, taking the initial compounds as $Sr(NO_3)_2$(SD fine 99.5%) ,Ti(100 mesh, Aldrich 99.7%) ,H_2O_2(30% ,SD fine) and Ammonia solution(25%, AR grade SD fine) has taken and the further process of the preparation is similar for these two powders. Initially the powders which we have taken in Stoichiometric proportion were dissolved in water then the required amount of Ti metal powder was added to a solution containing 70ml of H_2O_2 and 30 ml of Ammonia at 100^0C under constant stirring and yellow Gel was obtained after 12 h .These solution

was mixed with the initial solution, then citric acid was added to this solution in the ratio of 2:1 so that citrate will form. The P^H of the resultant solution was adjusted to 6-7 by adding Ammonia and the solution is heated. After some time, thick viscous liquid was obtained. At this stage ethylene glycol was added in the molar ratio of the citric acid to the ethylene glycol was 1:12. Then it is heated at 100^0C for 5-6 h. the temperature was increased to get precursor and this powder was grinded and calcined at various temperature for phase conformation. The calcined powders were mixed with molar ratio as required for the compositions and pressed into pellets of about 10mm diameter and 2mm thickness using Hydraulic press. Binders such as PVA are added in the process of pelletization and these pellets were prepared about 10mm diameter and 2mm thickness. These pellets were sintered in the range of 1160-1190^0C for 5 h to get final samples for measurements. The composition of the samples studied is given in table 1.

Table 1: compostion of samples studied and their compositions

S.NO	SAMPLE COMPOSITION	NOMENCLATURE
1	$Na_{1/2}Bi_{1/2}TiO_3$	NBT
2	(0.95)Na1/2Bi1/2TiO3+(0.05)$SrTiO_3$	NBST1
3	(0.90)Na1/2Bi1/2TiO3+(0.10)$SrTiO_3$	NBST2
4	(0.85)Na1/2Bi1/2TiO3+(0.15)$SrTiO_3$	NBST3
5	(0.80)Na1/2Bi1/2TiO3+(0.20)$SrTiO_3$	NBST4
6	(0.70)Na1/2Bi1/2TiO_3+(0.30)$SrTiO_3$	NBST5
7	(0.60)Na1/2Bi1/2TiO_3+(0.40)$SrTiO_3$	NBST6
8	(0.50)Na1/2Bi1/2TiO_3+(0.50)$SrTiO_3$	NBST7
9	(0.40)Na1/2Bi1/2TiO_3+(0.60)$SrTiO_3$	NBST8
10	(0.30)Na1/2Bi1/2TiO_3+(0.70)$SrTiO_3$	NBST9
11	(0.20)Na1/2Bi1/2TiO_3+(0.80)$SrTiO_3$	NBST10
12	(0.10)Na1/2Bi1/2TiO_3+(0.90)$SrTiO_3$	NBST11
13	SrTiO3	ST

X-ray diffraction peaks were obtained using Pan Analytical Xpert plus Diffract meter using Cu-Kα (1.54 Å) radiation. Spectra were recorded at room temperature in the range of $20^o \leq 2\theta \leq 80^o$ at a speed of 2^o/min. Densities of the sintered ceramics were measured by the Archimedes method using xylne (density 0.87gm / cm^3) as liquid media. SEM micrograph images of NBT, NBST and ST composites were obtained with ZEISS EVO18 (special edition) SEM and EDS spectra are obtained using Oxford EDS system which is attached to Zeiss SEM instrument

III. RESULTS AND DISCUSSION

SEM micrograph images of NBT, NBST and ST composites are shown in Figures 1 and 2. The homogeneous grain morphology is observed for composites. The pure NBT has spherical grain morphology. The apparent change is observed in the micro-structure of composites with high ST content. The cubic grain shape is observed for composites. The micro-structure of all the compositions indicates high density and low porosity. The grain size of composites changed asymmetrically with the composition. The grain size reduces with increase in ST content in NBST6, NBST7, NBST9 and NBST11 compositions. ST abounds in grain boundary regions which restricts the grain growth by preventing the ion migration.

The elemental analysis of NBT, ST and NBT-ST composites by EDS spectra is shown in Figures -3 and 4. The spectra shows that the composition of the present samples is as expected and the elements present in the prepared samples are Na, Bi, Sr, Ti and

O. The atomic and weight percentages of constituent ions or atoms obtained from EDS is similar to the proportions which are taken at the time of preparation and are listed in the Table-2. In EDS spectra X rays are emitted from various shells of different elements resulting in the radiation process. Na, Ti and O elements have radiations from K-shell. In Sr L-shell and in Bi, M-shell is radiative.

Table 2: weight percentage of different elements present in the synthesized samples

Sample	Na weight %	Bi weight %	Sr weight %	Ti weight %
NBT	5.09	54.96	-	22.33
NBST1	5.01	49.83	1.09	22.71
NBST2	4.85	46.52	2.67	23.20
NBST3	4.56	42.91	4.03	19.65
NBST4	4.18	37.90	6.28	20.76
NBST5	3.99	32.64	8.83	19.77
NBST6	3.37	30.54	16.41	20.80
NBST7	2.47	25.31	21.17	23.39
NBST8	2.22	19.40	26.62	23.78
NBST9	1.53	16.51	31.05	24.13
NBST10	1.01	8.94	34.62	24.80
NBST11	0.46	4.94	42.47	25.03
ST	-	-	32.77	44.38

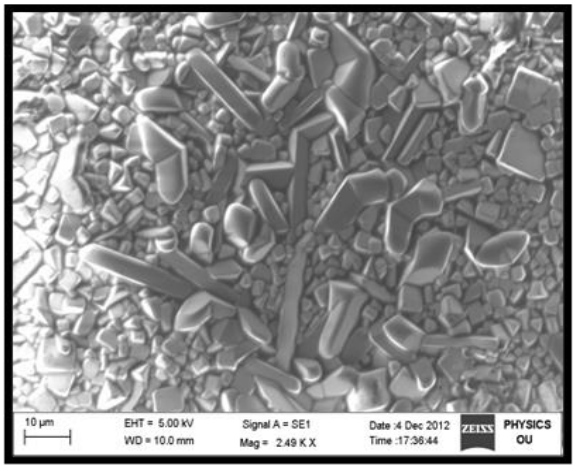

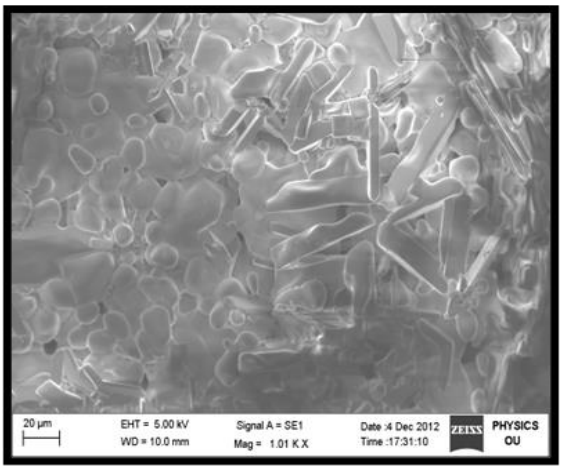

Figure 3 SEM micrographs of NBT-ST composites

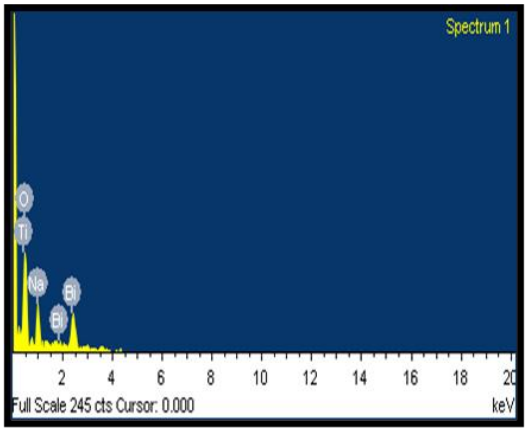

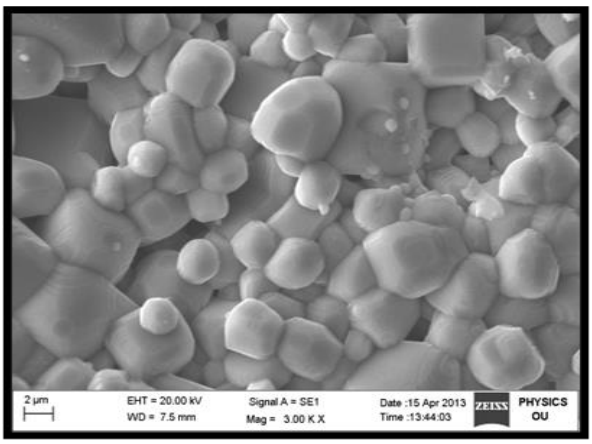

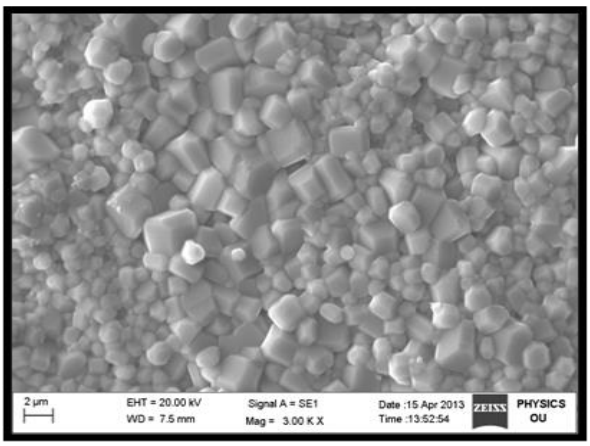

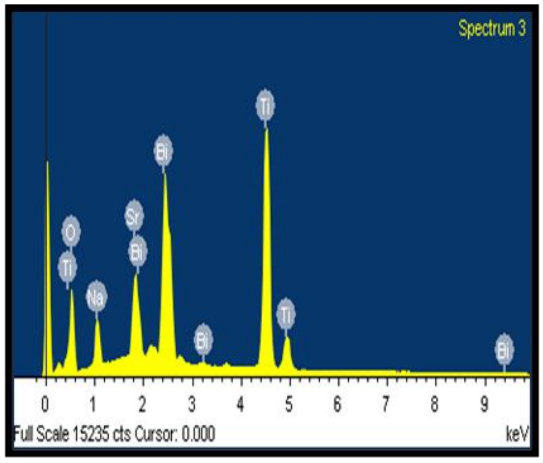

Figure-3:EDS of sintered NBT ST composites

Powder diffractometer the X-ray diffractograms obtained ares shown in Figure-5.

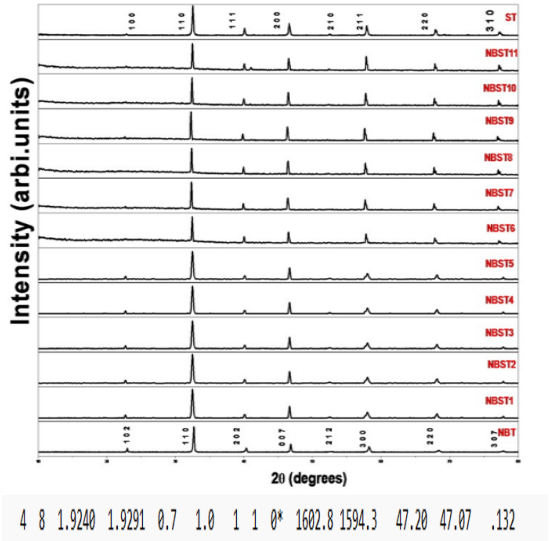

4 8 1.9240 1.9291 0.7 1.0 1 1 0* 1602.8 1594.3 47.20 47.07 .132

Figure-5: X-ray diffractograms of NBT-ST coomposites

By using POWD software and least square fitting, the lattice parameters are calculated. Densities of the ceramic composites are measured by Archimedes principle and are compared with X-ray densities. Lattice parameters of pure NBT are a=5.49Aº and c=13.60Aº. The lattice parameter of ST is a=3.90Aº. The lattice parameters of composites are showing little change indicating the existence of individual phases. The ratio of experimental to theoretical density is more than 92% for the present samples. The pertinent data is summarized in table 3.

Table 3: Lattice paramenters, density and particle size obtained form XRD data

Sample	Relative density	Particle size(nm)	Rhombohedral a(A°)	c(A°)	Theoretical density
NBT	97	45.97	5.496	13.606	5.90
(0.95NBT+0.05ST) NBST1	95	53.05	5.498	13.562	5.22
(0.90NBT+0.10ST) NBST2	95	49.26	5.498	13.586	5.49
(0.85NBT+0.15ST) NBST3	90	53.08	5.467	13.562	5.43
(0.80NBT+0.20ST) NBST4	91	69.08	5.498	13.262	5.69
(0.70NBT+0.30ST) NBST5	93	84.98	5.498	13.562	5.87
(0.60NBT+0.40ST) NBST6	94	105.80	5.500	13.562	5.89
(0.50NBT+0.50ST) NBST7	93	105.23	5.500	13.583	5.86
(0.40NBT+0.60ST) NBST8	95	105.35	5.500	13.564	5.89
(0.30NBT+0.70ST) NBST9	97	105.16	5.501	13.587	5.89

Williamson-Hall plots [11] are a graphical method used in materials science and crystallography to analyze the broadening of X-ray diffraction (XRD) peaks. This method helps separate and quantify the contributions of crystallite size and lattice strain to the overall peak broadening observed in diffraction patterns, providing valuable insights into the microstructural characteristics of materials.

When X-rays are diffracted by a crystalline material, the resulting peaks in the XRD pattern may broaden due to two primary factors:
Crystallite Size: Smaller crystallites tend to scatter X-rays over a broader range of angles, leading to peak broadening.

Lattice Strain: Internal stresses or defects within the crystal lattice can cause variations in the interplanar spacing, resulting in additional peak broadening.

The Williamson-Hall approach combines these two contributions into a single analysis. The method is based on the relationship between the full width at half

maximum (FWHM) of the diffraction peak and the crystallite size and strain. The fundamental equation used in Williamson-Hall plots is:

$\beta\cos\theta=\frac{K\lambda}{D}+4\varepsilon\sin\theta$

Where: β = FWHM of the diffraction peak (in radians), θ = Bragg angle corresponding to the diffraction peak, K = Shape factor, typically around 0.9 for spherical crystallites, λ = Wavelength of the X-ray radiation used, D = Average crystallite size, ε = Lattice strain.

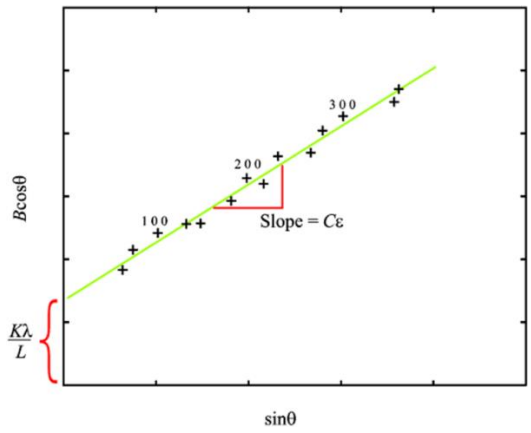

Figure 6: Willamson Hall Plot of NBT samples

Table 4: Crystallite sizes and micro stain of all NBT-ST composite materials

S.N0	Samples	Crystallite Size(D)	Strain(ε)
1.	NBT	39.16	0.072105
2.	NBST1	20.03	1.4623175
3.	NBST2	30.11	0.0020725
4.	NBST3	19.26	0.01459
5.	NBST4	14.65	0.1212675
6.	NBST5	10.60	0.0864475
7.	NBST6	12.93	0.3159725
8.	NBST7	12.09	0.3621225
9.	NBST8	17.99	0.0456175
10.	NBST9	21.42	0.058305
11.	NBST10	20.58	0.0731575
12.	NBST11	23.74	0.0637375
13.	ST	12.69	0.04153

The Goldschmidt tolerance factor (t) is defined by the following formula [10]:

$t=\frac{rA+rB}{\sqrt{2}(rB+rO)}$

Where in ABO_3 material:

r_A = Ionic radius of the A-cation; r_B = Ionic radius of the B-cation; r_O = Ionic radius of the oxygen anion

The value of t provides insight into how well the ions in a perovskite structure fit together, predicting whether the structure will remain cubic or distorted. If $t \approx 1$ (typically $0.9 < t < 1$): The material is likely to form a cubic perovskite structure, where the cations and anions are arranged in a stable configuration without significant distortion. If the value of $t < 1$then the A-cation is too small to perfectly fit the ideal cubic structure. As a result, the perovskite structure will typically distort, adopting tetragonal, orthorhombic, or rhombohedral symmetry. A tolerance factor less than 1 often corresponds to a "compressed" structure where the Bsite cation and the oxygen octahedra become distorted. If tolerance factor $t > 1$ suggests that the A-cation is too large for the lattice, which causes the perovskite structure to become unstable and adopt alternative structures, such as hexagonal or non-perovskite structures. A-site ions in the present compositions are a combination of Na^+, Bi^{3+}, and Sr^{2+} depending on the composition. The B-site is only occupied by Ti^{4+} in all cases. The relevant ionic radii (Shanon ionic radii in Angstrom units) [8] are Na^+ (A-site) = 1.39 Å; Bi^{3+} (A-site) = 1.17 Å; Sr^{2+} (A-site) = 1.44 Å; Ti^{4+} (B-site) = 0.605 Å O^{2-} (oxygen) = 1.40 Å. The calculated values of NBT composites are shown in table 5.

Table-5: Tolerance factor of Samples

Samples	r_A(Å)	r_B(Å)	r_O(Å)	t
NBT	1.28	0.605	1.40	0.946
NBST1	1.288	0.605	1.40	0.948
NBST2	1.296	0.605	1.40	0.951
NBST3	1.304	0.605	1.40	0.954
NBST4	1.312	0.605	1.40	0.956
NBST5	1.328	0.605	1.40	0.962
NBST6	1.344	0.605	1.40	0.968
NBST7	1.360	0.605	1.40	0.973
NBST8	1.376	0.605	1.40	0.979
NBST9	1.392	0.605	1.40	0.985
NBST10	1.408	0.605	1.40	0.990
NBST11	1.424	0.605	1.40	0.996
ST	1.44	0.605	1.40	1.002

REFERENCES

[1] G.A.Smolenskii, V.A.Isupov, R.I.Agranovskaya, N.n. Kainik, Sov. Phys.Solid state 2(1961) 2651.

[2] Bahuguna Saradhi B V, srinivas K, Prasad G, Suryanarayana SV,Bhimashankaram T(2003) Material Sci Eng B 98:10

[3] Zhen Fu, Ranqing Zhu, DI WU, Aidong Li(2009) J.sol-gel Technol 49:29-34

[4] Leow Chun Yan, Junian Hassan ,Mansor Hashmir, Wong Swee Yin, Tan Foo Khoon and Wong Yick Jeng14(7)(2011) World Applied Sciences Journal 1091-1094.

[5] Barker,A.S. and Tinkham, Jr.,M.,Phys.Rev.B(1962)125,1527-1530.

[6] Dunmin Lin, K.W.Kwok,H.L.W.Chan(2009) Jr.of alloys and compounds 310-315

[7] Langford, J.I. and Wilson, A.J.C. (1978). Journal of Applied Crystallography, 11, 102-113.

[8] R.D. Shannon, *Acta Cryst.* A32 751-767 (1976).

[9] M.Khan A Mishra Shukla and P.Sharma, "X-ray analysis of BaTiO3 ceramics by Williamson-Hall and size strain plot methods" inA *IP Conference Proceedings*, 2019 , Vol. 2100 , No. 1 : AIP Publishing LLC, p. 020138 https://doi.org/10.1063/1.5098692

[10] V. M. Goldschmidt *Naturwissenschaften*, 1926, 14 , 477 —485